Research on Engineering Structures & Materials
www.jresm.org
Research Group

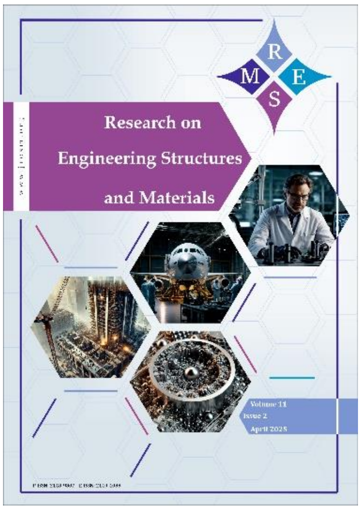

Experimental investigation on the shear behavior of steel fibre reinforced concrete deep beams with strategic circular web openings

Arun Kumar C J, S Rajendra, Kumar K, G R Manjunath

Online Publication Date: 30 August 2026

URL: http://www.jresm.org/archive/resm2026-2099st0802rs.html
DOI: http://dx.doi.org/10.17515/resm2026-2099st0802rs

Journal Abbreviation: *Res. Eng. Struct. Mater.*

Research on Engineering Structures & Materials
www.jresm.org
MIM Research Group

Research Article

Experimental investigation on the shear behavior of steel fibre reinforced concrete deep beams with strategic circular web openings

Arun Kumar C J [*,1,2,a], S Rajendra [1,b], Kumar K [1,c], G R Manjunath [3,d]

[1]*Dept. of Civil Eng., Nagarjuna College of Engineering & Technology, Bengaluru, Karnataka, India*
[2]*Dept. of Civil Eng., SJC Institute of Technology, Chickballapur, Karnataka, India*
[3]*Dept. of Civil Eng., Sapthagiri College of Engineering, Bengaluru, Karnataka, India*

Article Info

Article History:

Received 02 Aug 2026

Accepted 25 Aug 2026

Keywords:

RCC deep beam;
Circular web openings;
Crimped steel fibre;
Shear capacity;
Load transfer mechanism;
Structural performance

Abstract

Building services often require openings in RCC deep beams, which can disrupt the internal load-transfer mechanism and adversely affect shear performance. This study experimentally and theoretically investigates the effect of circular web-opening location on the shear behavior and load-carrying capacity of RCC deep beams, with particular emphasis on openings positioned in the tension and compression zones. A total of 45 deep beam specimens representing 15 configurations, comprising solid deep beams (SDB), deep beams with openings in the compression zone (DB-C), and deep beams with openings in the tension zone (DB-T), incorporating crimped steel fibre (CSF) dosages of 0%, 0.25%, 0.50%, 0.75% and 1.00%, were tested under two-point loading. The results showed that compression-zone openings caused less reduction in load-carrying capacity than tension-zone openings. At 0% CSF, the capacity loss relative to SDB was 2.4% for DB-C and 7.3% for DB-T, while at 1% CSF, the corresponding losses were 2.8% and 6.7%, respectively. At 1% CSF, the first-crack load increased by 35.1-41.9% and the ultimate load 9.4-10.5% compared with the corresponding specimens without CSF. DB-C exhibited 9.1% higher first-crack load and approximately 4.2% higher ultimate load than DB-T at 1% CSF. The theoretical predictions agreed reasonably well with the experimental results, with variation of approximately 0.6-10.8%.

1. Introduction

High-rise structures with long infrastructural spans utilize deep beams, acting as the fundamental backbone to absorb and distribute heavy load. To efficiently absorb immense structural demands, heavy duty buildings and bridges rely on deep profile beams to counteract vertical deflections and bending stress. A deep beam is a structural element whose depth is so significant relative to its length (span) that it behaves more like a solid wall or an upright tied arch than a traditional, slender beam. Openings in such beams with greater depth are commonly provided in modern construction scenarios like buildings, bridges etc., to accommodate essential services like electrical installations, AC ducts, drainage pipes etc., and sometimes for accessibility. Such openings are usually embedded in the beam web with required shape, size and strategic position relying on the service requirements. Two major opening shapes are commonly adopted (circular and rectangular) with circular opening**s** demonstrating better performance in stress distribution and improved serviceability [11,19]. In such deep beams it is essential to assess the structural behavior along with ultimate strength since the presence of a circular opening disrupts the load transfer mechanism within the beam [6]. It is widely recognized that the classical elastic beam theory fails to accurately

*Corresponding author: arubcjgowda@gmail.com
[a]orcid.org/0000-0001-8774-9775; [b]orcid.org/0000-0003-1709-0674; [c]orcid.org/0000-0002-0281-0379; [d]orcid.org/0009-0006-4956-0887
DOI: http://dx.doi.org/10.17515/resm2026-2099st0802rs

describe the behavior of these beams as their behavior is regulated by non-linear stress distribution and direct load transfer through compression struts instead of conventional flexure action in accordance with the load-transfer mechanism described by Strut-and-Tie Model (STM). This adverse effect primarily arises from improper load-path-oriented opening in the deep beam. The largest crack width at ultimate failure is encountered due to opening center positioned within the critical shear zone rather than any other portion in deep beams. The web openings in the deep beam should not be positioned closer to the vertical edges all around the beam since higher loading may reduce structural integrity causing premature failure. Also, the deflection in such beam with greater depth having opening is predominantly influenced by shear effect. Hence, positioning a web opening within the high-shear region interrupts the critical load path, significantly reducing beam stiffness and ultimate strength.

To locate optimum load-path-oriented position of circular web opening, a comprehensive load transfer mechanism is essential with following factors influencing the structural behavior pertaining to deep beam i.e., span to its depth ratio, cross section details, main and web reinforcements, properties of concrete, type and position of loading, type and shape of web opening etc. Web openings in beams of greater depth also interrupt the continuity of shear reinforcement and disrupt the formation of effective struts, which can cause a sudden drop in shear capacity and lead to premature shear failure, thereby adversely affecting the overall structural performance. Under such scenarios it is not feasible to place steel in the line of opening especially shear, main and side face reinforcement. Externally bonded steel sheets, or steel fiber infills effectively restore the continuity of shear transfer mechanism within the disturbed region by improving tensile stress transfer and bridging developing cracks [1,18].

Use of closely spaced and uniformly dispersed fibre in concrete reduces the effect of openings in the beams of greater depth. Fiber reinforcement, such as the use of CFRP or the, introduction of steel fibres is much effective for enhancing the shear performance of reinforced concrete beams of greater depth approximately by 35% at 0.75% fibre content when the openings are provided in compression zone and decreases the development of cracks which are formed in concrete primarily due to openings [2,14, 18]. Interface adhesion between steel fibre and concrete also enhance the stress transfer with optimum dosage of up to 1% [18]. Variety of such fibres are available with most widely manufactured and available is crimped type of steel fibre. The incorporated crimped type of steel fibre also features more in its presence in the concrete by restricting crack growth, improving tensile strength, and acting as shear reinforcement etc. Due to these advantages, CSF is an optimal additive for the concrete beams with larger depths. Key findings from previous studies are summarized below:

- Circular openings are more effective than rectangular, square, or other geometries [19].
- Increasing the steel fibre content up to 2% in the concrete leads to improvement in shear carrying capacity, reduced deflection, cracks with improvement against failure [15].
- Despite previous studies on deep beams with web openings and fibre-reinforced concrete, the combined influence of circular web openings and crimped steel fibres (CSF) on shear behavior remains insufficiently investigated. CSF was selected for its crimped geometry and enhanced mechanical anchorage, which promote crack bridging within the concrete matrix.
- Limited attention has been given to the combined influence of load-path-oriented circular opening placement and varying CSF dosages, particularly with respect to identifying an optimum opening position that minimizes disruption to the principal load-transfer path.

The present study explores the influence of load-path oriented circular web opening on the structural performance pertaining to deep beams, identifies the most favorable location of openings to satisfy service requirements while mitigating disruption to the natural load transfer path. This study also assesses the potential of crimped steel fibres in mitigating the adverse effect of circular web opening on the overall performance pertaining to deep beams. Therefore, the present study aims to experimentally investigate the influence of load-path-oriented circular web openings location in the compression and tension zones on the shear behavior and load-carrying capacity of RCC deep beams. The study further evaluates the effectiveness of CSF at different dosages in minimizing adverse effects of web openings and improving the ultimate load-carrying behavior reducing the cracks and deflection.

2. Methodology

To ascertain the influence of openings, a total of 45 deep beam specimens representing 15 configurations were fabricated and tested. The specimens had an overall length of 750 mm, a width of 75 mm and the depth of 325 mm, and were classified into three beam types: having openings at compression zone (DB-C) and tension zone (DB-T) along with solid specimen without openings (SDB) were fabricated and tested to failure under a gradually applied symmetrical two-point loading system using 1000 kN capacity universal testing machine (UTM). The tests were conducted under load-controlled conditions at a loading rate of 0.5 kN/s, with observations recorded at 10 kN load increments. Mid-span deflection was measured using a dial gauge with a least count of 0.01 mm.

Table 1. Summary of tested deep-beam specimens

Beam configuration	CSF volume fraction (%)	Replicates per CSF level	Total Specimens
SDB	0, 0.25, 0.50, 0.75, 1.00	3	15
DB-C	0, 0.25, 0.50, 0.75, 1.00	3	15
DB-T	0, 0.25, 0.50, 0.75, 1.00	3	15
			Total 45

The following experimental procedure is adopted:

- The physical and engineering properties of materials employed for concrete matrix preparation were evaluated in the laboratory as prescribed in respective Indian Standard (IS) code provision.
- Proportioning the concrete mix for M20 grade, designed in compliance with the recommended IS 10262:2019 by incorporating various volume fractions of CSF to cast the test specimens for compression and shear strength test.
- The deep beams were designed with longitudinal, vertical, and side-face reinforcement.
- Concrete beams of greater depth specimens were cast with the help of wooden formwork having specified measurements with provision of circular web opening of 75 mm diameter at designated position along with standard concrete cubes for compression test.
- To evaluate the compressive strength, a total of thirty concrete cubes were cast, comprising three specimens for each of the five CSF contents at each testing age of 7 and 28 days.
- After the specified curing period, laboratory tests were conducted for cast crimped steel fibre concrete cubes and beams of specified measurements for compressive strength using 2000 kN capacity digital compression testing machine, and shear carrying capacity pertaining to deep beam of circular web opening made in compression zone (DB-C), opening made in tension zone (DB-T) and SDB is conducted using 1000 kN capacity UTM.
- Results are analyzed and compared with theoretical model (Professor F. K. Kong's model) to validate the experimental work.

3. Material Properties

The following constituent materials, possessing the required physical and engineering properties are employed in the preparation of specified specimens:

3.1 Cement

53 Grade Ordinary Portland Cement (OPC) having specific gravity 3.11 is used for proportioning cement concrete of grade M20. Fine Aggregates: Manufactured sand as fine aggregates pertaining to zone II with specific gravity of 2.60 and a fineness modulus of 3.15. The measured silt content was 0% and moisture content was 4%. Coarse Aggregates: Considering the presence of CSF and limited beam width of 75 mm, 10 mm downsized coarse aggregate with a specific gravity of 2.72 and a bulk density of 1640 kg/m^3 was used for preparing the concrete. Bore well water which is free from dust and dirt having pH 7.2 conforming to IS 456:2000 was used for mixing and curing.

A superplasticizer: RHEOBUILD SP1, manufactured by BASF Construction Chemicals (India) Pvt. Ltd., which is sulphonated naphthalene-formaldehyde polymer-based admixture with a specific gravity of 1.15 was included as high-range water-reducing superplasticizer to enhance the workability especially during mixing of concrete along with CSF which are more vulnerable to balling effect.

3.2 HYSD Steel Bars

For reinforcement 2 HYSD bars of 12 mm diameter, conforming to Fe 500 grade are provided as the main tension steel. In addition, 6 # 8 mm in 3 layers are provided as horizontal side face reinforcement. The physical properties of reinforcement bars obtained from tensile test are presented in the table 2.

Table 2. Physical test results of HYSD bars

Diameter (mm)	Sectional weight (kg/m)	Yield strength (N/mm^2)	Ultimate strength (N/mm^2)	Elongation (%)
12	0.863	515	590	16.05
8	0.373	510	588	16.55

CSF (crimped steel fibre) possessing an aspect ratio of 60 having a length of 60 mm and 1 mm diameter with a tensile strength of 1150 MPa with the density of 7850 kg/m^3 is selected to achieve enhanced shear resistance and improved crack bridging action.

4. Concrete Mix Design

The concrete mix associated with M20 grade was proportioned in compliance with the guidelines of IS 10262:2019 for concreting in mild exposure conditions. To facilitate consistent fibre dispersion and to control balling effect, superplasticizer is added with nominal maximum size of aggregates was limiting to 10 mm, enhancing the cohesiveness and fresh state workability of fibre reinforced concrete.

CSF was incorporated as a discrete reinforcing phase at volume fractions ranging from 0% to 1%, in increments of 0.25%. The quantities of the concrete constituents presented in Table 3 are expressed in kg/m^3. The water-cement ratio and superplasticizer dosage were maintained constant at 0.45 and 7.20 kg/m^3, respectively, for all mixtures. The superplasticizer facilitated fibre dispersion and reduced the possibility of fibre balling. The measured 4% moisture content of the fine aggregate was accounted for when determining the net mixing water. The workability of the fresh concrete mixtures was evaluated using the slump test in accordance with IS 1199 (Part 2): 2018. The absolute-volume method was used to maintain a total concrete volume of 1 m^3. Accordingly, the sum of the absolute volumes of cement, water, superplasticizer, CSF, fine aggregate and coarse aggregate was maintained as:

$$V_c + V_W + V_{sp} + V_{CSF} + V_{FA} + V_{CA} = 1.00\ m^3 \quad (1)$$

The absolute volume of each constituent was calculated using:

$$V_i = \frac{m_i}{SG_i\ x\ 1000} \quad (2)$$

Where V_i, m_i and SG_i represent the absolute volume, mass and specific gravity respectively, of constituent i. As the CSF volume fraction increased, an equivalent volume was deducted from the combined aggregate volume, while the cement content, water content and superplasticizer dosage were maintained constant. The fine and coarse aggregate quantities were adjusted by maintaining approximately 39% and 61%, respectively, of the total aggregate volume. The resulting quantities of all constituents are presented in Table 3.

Table 3. Mix proportions and slump values of M20 concrete containing different CSF volume fractions

Crimped steel fibre (%)	Cement (kg/m^3)	Fine aggregates (kg/m^3)	Coarse aggregates (kg/m^3)	Water (kg/m^3)	Superplasticizer (kg/m^3)	CSF (kg/m^3)	Slump (mm)
0	380.88	709.90	1161.61	171.40	7.20	0	89
0.25	380.88	707.37	1157.46	171.40	7.20	19.63	81
0.50	380.88	704.83	1153.31	171.40	7.20	39.25	79
0.75	380.88	702.30	1149.16	171.40	7.20	58.88	74
1.00	380.88	699.76	1145.01	171.40	7.20	78.50	71

The slump decreased progressively from 89 mm for the control mixture to 71 mm at 1% CSF, corresponding to a reduction of approximately 20.2%. This reduction was attributed to the increased surface area, internal friction and interlocking effects introduced by the fibres. Nevertheless, all mixtures exhibited adequate workability for placement and compaction. A representative view of distribution of CSF in the fresh concrete mix is shown in Fig. 1, indicating adequate fibre dispersion without noticeable agglomeration.

Fig. 1. Distribution of CSF in the concrete mix

5. Design of RCC Deep Beam

Design data:

- Length of beam, L = 750 mm
- Depth of beam, D = 325 mm,
- Width of beam, b = 75 mm
- Support width = 100 mm
- Clear span = 550 mm
- Diameter of circular web opening = 75 mm

Effective depth, d = 325 – 20 – 8 – (12/2) = 291 mm, considering a clear cover of 20 mm, an 8 mm stirrup and 12 mm main bar. According to IS 456:2000, effective span of deep beam is smaller of:

- Centre-to-center distance between supports = 750 – 100 = 650 mm
- 1.15 times clear span = 1.15 (550) = 632.5 mm
- Consider smaller of above, effective span (l) = 632.5 mm

Effective span by overall depth ratio (l/D) = 632.5/325 = 1.94 < 2.0; therefore, the specimen satisfied the IS 456:2000 criterion for a simply supported deep beam. For the symmetrical two-point loading system applied at one-third points of effective span, the shear span is,

- a = 632.5/3 = 210.83 mm

Therefore, shear span to effective depth ratio = a/d = 0.72. Reinforcement details:

- Main tension steel: 2#12 mm diameter HYSD bars.
- Horizontal Side-face reinforcement: #8mm @ 95mm c/c on both faces in 3 layers.

The circular opening interrupted one layer of side-face reinforcement in both DB-C and DB-T specimens. However, two-legged 8 mm diameter stirrups at 230 mm c/c were provided as shear reinforcement in all three beam configurations, namely SDB, DB-C and DB-T. The CSF provided supplementary crack-bridging resistance in the vicinity of the openings [19].

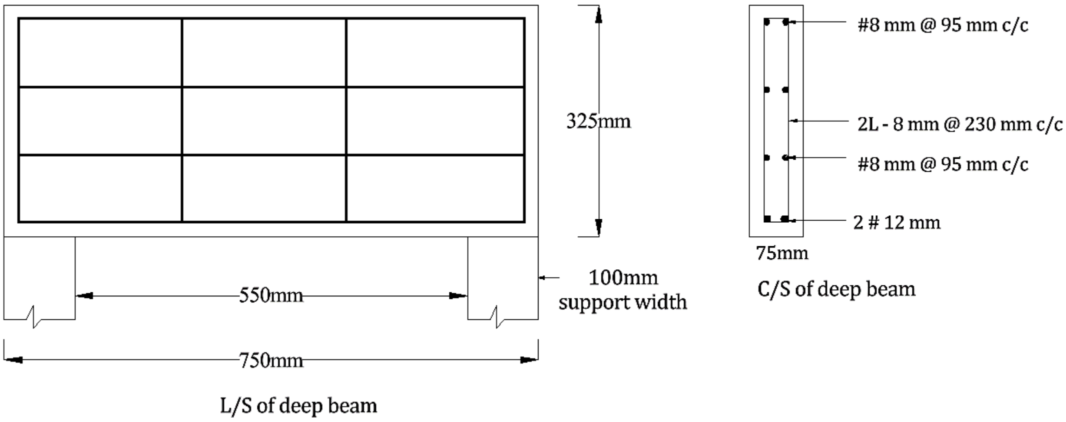

Fig. 2. Schematic illustration of longitudinal and cross-sectional reinforcement details of the deep beam (SDB)

Positioning (locating) of openings in the deep beam: While casting the concrete beams circular web openings were introduced at two different locations in the beam having larger depths: in compression zone (DB-C), in tension zone (DB-T) using PVC pipes of 75 mm outer diameter at the designated locations and the same is removed after the concrete had attained its initial set. The designated location of web openings was oriented based on load transfer mechanism in the deep beams. During the loading process, the load is transferred from source point to supports primarily through compression strut. To minimize the disruption of this load transfer mechanism, the openings are located outside the principal load path within the disturbed region. Accordingly, the openings in web are provided at compression and tension zone. The provision of openings and its size depends on the load-transfer zones and the corresponding geometrical parameters, as illustrated in Fig. 3 and 4.

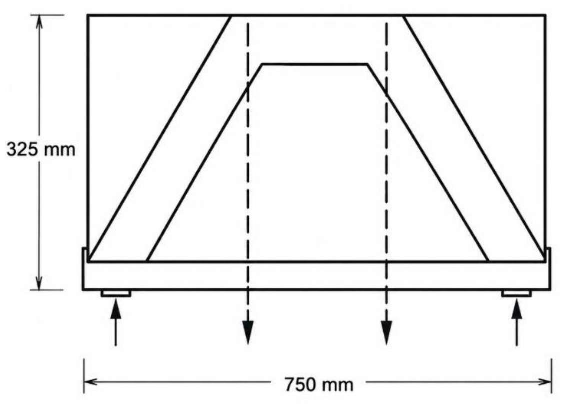

Fig. 3. Load transfer path in deep beam

The failure modes are categorized into two groups:

- Failure associated with compressing of inclined concrete member also called as inclined compression failure
- Bending (flexural) failure, which are represented by means of failure of horizontal concrete tie member.

As illustrated in fig. 4 load path with quadrants 1 and 3 signifies the primary load transfer regions, as 1 and 3 quadrants located adjacent to the loading and support zones. These regions transfer the principal compressive forces from the point of load application to the supports and hence play an important role in structural performance pertaining to deep beam. In contrast, 2 and 4 quadrants are considered as unloading path or comparatively less stressed regions away from loading path of beam and where actually the openings are preferred.

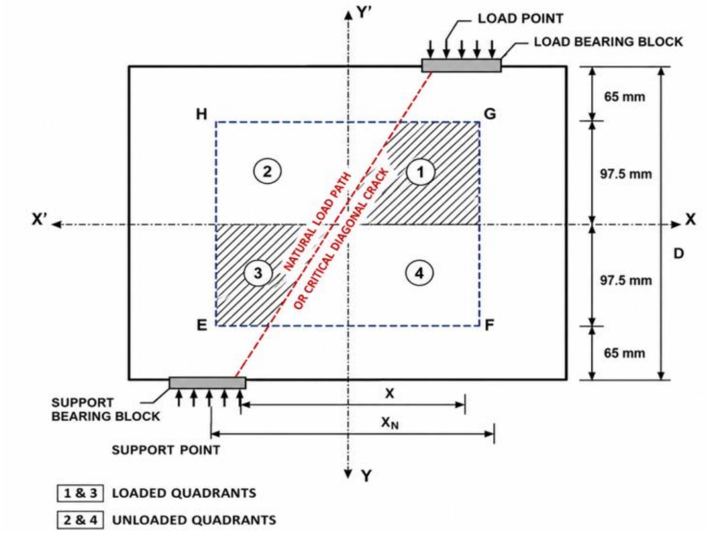

Fig. 4. Loading path with quadrants and geometrical parameters in deep beam

Considering the eccentricity in x and y direction (i.e., ex and ey) from center of opening and to the center of diagonal load path plays an important role in choosing the diameter of the opening in the deep beams. However, it is limited [19]:

- ex ≤ Xn/4
- ey ≤ 0.6D/4
- $X_{net} = (X_N - a_1X)$ $\quad e_x \leq X_N/4$
- $Y_{net} = (0.6D - a_2D)$ $\quad e_y \leq 0.6D/4$

Where: X_N = Distance from support point to right edge, X = Distance from support point to load point, D = Overall depth of the member, K_1 & K_2 = Coefficient for critical diagonal = 0.23 & 0.55 respectively. a_1 & a_2 = Opening location parameter = 0.60 & 0.23 respectively. e_x, e_y = Eccentricities of opening center from critical diagonal.

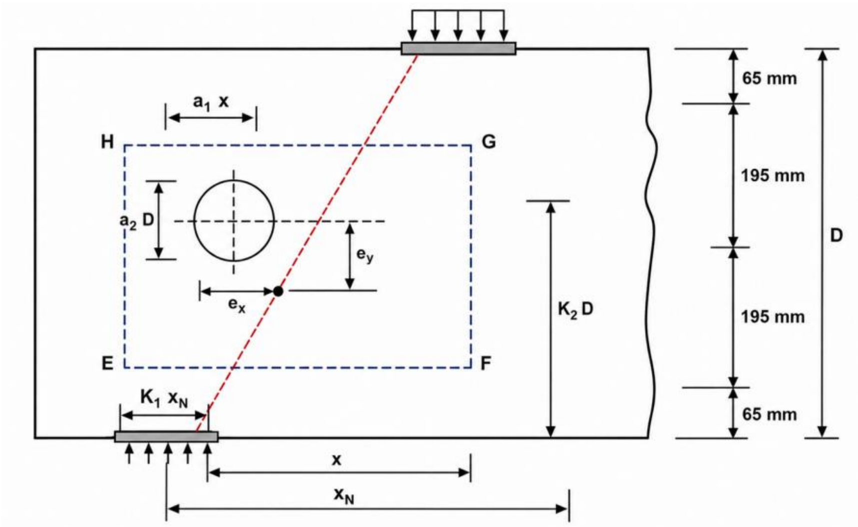

Fig. 5. Schematic representation of the opening location in the deep beam

6. Experimental Work

Standard concrete cubes (150 mm × 150 mm × 150 mm) containing 0%, 0.25%, 0.50%, 0.75%, and 1% CSF were tested using a 2000 kN capacity compression testing machine. The test was performed and reported as per the technical reference IS 516:2021and IS 456:2000 for 7 days and 28 days curing period. The equivalent cylindrical compressive strength was estimated from the cube compressive strength using a conversion factor of 0.80, i.e., fc =0.80fck, for comparison with cylindrical-based design provisions.

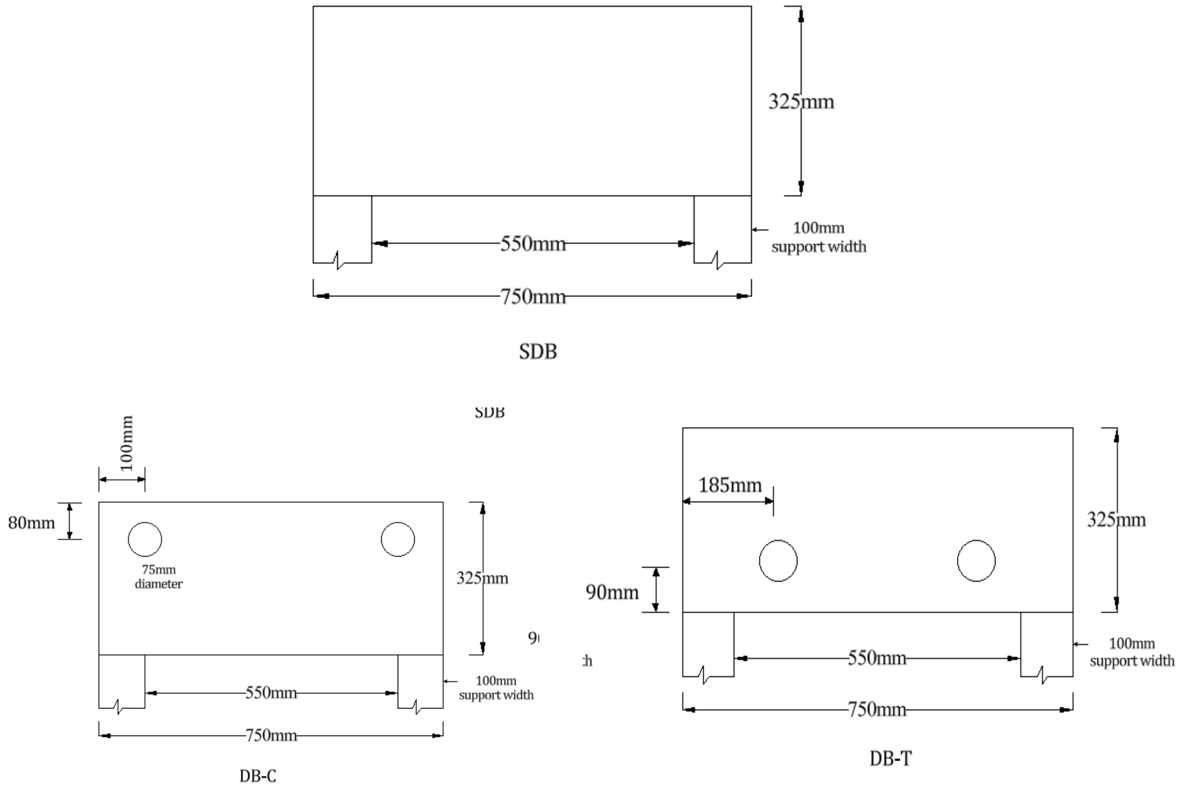

Fig. 6. Schematic representation of deep beam – SDB, DB-C and DB-T respectively

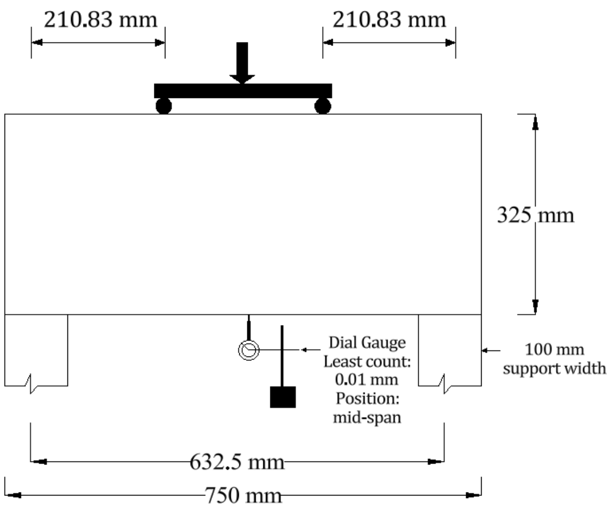

Fig. 7. Schematic representation of symmetric two-point loading setup and dial-gauge position at mid-span

The Shear behavior of the deep-beam specimens was evaluated under symmetric two-point loading applied at the one-third points of the effective span. All specimens were tested after 28 days of curing using a 1000 kN capacity universal testing machine in accordance with the applicable provisions of IS 516 (Part 1):2021.

The dimensions of all the specimens were measured prior to testing and were subjected to incremental loading until failure. During testing the first-crack load, ultimate load, crack initiation with its propagation and extension towards the openings were recorded. The maximum mid-span deflection was measured using a dial gauge with a least count of 0.01 mm. The dial gauge was mounted on an independent rigid stand, with spindle positioned vertically in contact with the beam soffit at the exact mid-span, as shown in Fig. 7. Following type pertaining to deep beams with 0%, 0.25%, 0.50%, 0.75% and 1% steel fibre content are tested in the experiment work:

- Solid deep beam without openings (SDB)
- Deep beam with circular openings at compression zone (DB-C).
- Deep beam with circular openings at tension zone (DB-T).

Table 4. Measured cube and equivalent cylindrical compressive strengths of concrete with varying CSF content

Percentage of crimped steel fibres (%)	Average density of concrete (kN/m³)	Average cube Compressive strength (N/mm²) f_{ck}	Average cylindrical compressive strength (N/mm²) $f_c = 0.80f_{ck}$
0	23.96	22.00	17.60
0.25	24.18	24.10	19.28
0.50	24.37	27.50	22.00
0.75	24.61	31.85	25.48
1.00	24.98	33.75	27.00

7. Results and Discussion

The laboratory investigation was performed to ascertain the influence of load-path oriented circular opening position on their load carrying behavior. A comparative assessment was performed for solid beam without opening (SDB), deep beam with circular opening in compression zone (DB-C) and deep beam with circular opening made in tension zone (DB-T). Each specimen responses for first crack load, the ultimate load, deflection along with crack propagation were analyzed. The numerical results represent the arithmetic means of three replicate specimens for each configuration and CSF volume fraction. Load values were rounded to the nearest 1 kN, while deflection values were reported to two decimal places.

7.1 Load Deflection Behavior of Solid Deep Beam (SDB)

Table 5 presents the experimental results indicating the addition of steel fibers enhance the structural response by delaying the first-crack load, increasing ultimate load capacity, and reducing maximum deflection. The addition of crimped steel fibres significantly enhances the behavior of solid deep beam (SDB).

Table 5. Load – Deflection of solid deep beam without opening for various CSF content

Percentage of crimped steel fibres (%)	Number of specimens	SDB		
		Mean First Crack Load (kN)	Mean Ultimate Load (kN)	Mean Maximum Deflection (mm)
0	3	74	164	2.50
0.25	3	80	168	2.46
0.50	3	85	170	2.41
0.75	3	98	178	2.36
1.00	3	100	180	1.80

The first crack load obtained for solid deep beam increased from 74 kN to 100 kN for the control specimen representing an improvement of approximately 35% at 1% CSF content. Similarly ultimate load also increases from 164 kN to 180 kN representing an improvement of approximately 9.8% at 1% CSF content. This higher improvement in first-crack load compared with ultimate load indicates that the primary contribution of the fibres was associated with crack initiation and crack-control mechanisms. CSF which are randomly distributed, bridge developing microcracks and transfer tensile stresses across the cracked concrete matrix, thereby delaying the formation and propagation of visible cracks. At 1% steel fibre dosage, the maximum deflection was reduced by about 28% compared to control specimen

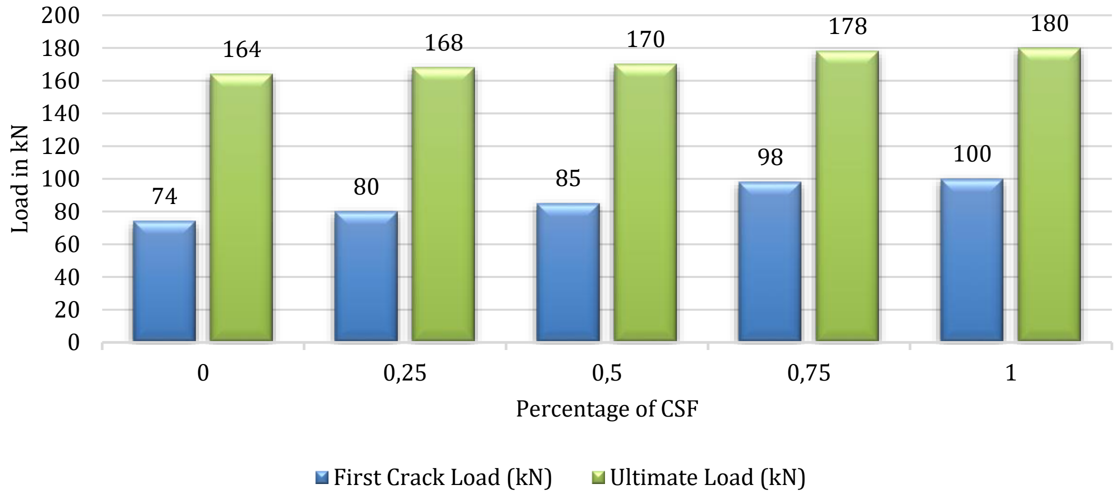

Fig. 8. First crack load and ultimate load for SDB

7.2 Load Deflection Behavior pertaining to deep beam with Circular Opening in Compression Zone (DB-C)

The behavior pertaining to deep beam with circular web opening in compression zone (DB-C) also demonstrated a progressive improvement with increase in crimped steel fibre content. Compared to the control specimen the first crack load increased from 68 kN to 96 kN representing an increase of about 41.2% for 1% fibre. Similarly, the ultimate load also increases from 160 kN to 175 kN with an improvement of 9.4% approximately compared to control specimen. The maximum deflection is reduced by 24% by adding up to 1% fibre content in an increment of 0.25%.

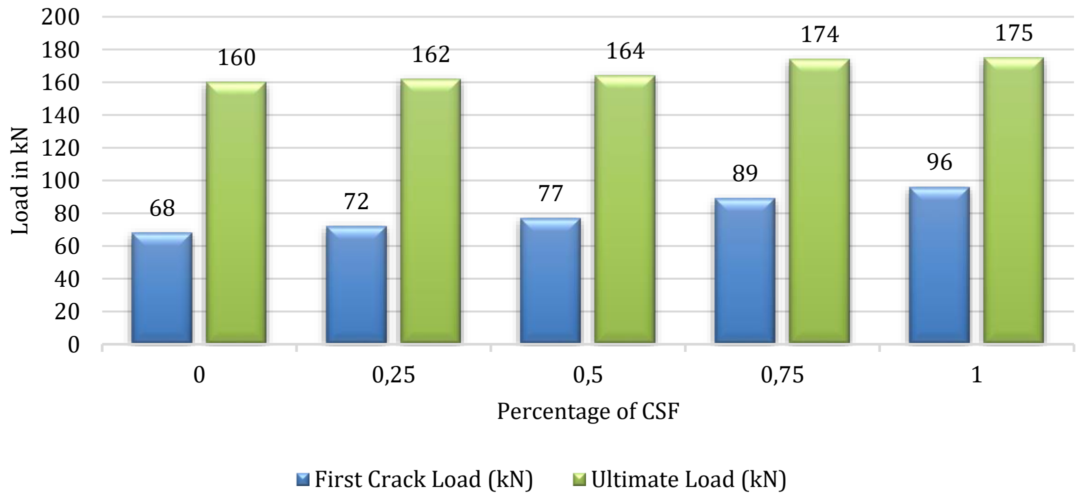

Fig. 9. First crack load and ultimate load for DB-C

Table 6. Load – Deflection pertaining to deep beam with opening in compression zone for various CSF content

Percentage of crimped steel fibres (%)	Number of specimens	DB-C		
		Mean First Crack Load (kN)	Mean Ultimate Load (kN)	Mean Maximum Deflection (mm)
0	3	68	160	2.58
0.25	3	72	162	2.52
0.50	3	77	164	2.29
0.75	3	89	174	2.14
1.00	3	96	175	1.96

7.3 Load Deflection Behavior pertaining to deep beam with Circular Opening in Tension Zone (DB-T)

The DB-T specimens also exhibited a comparable response for addition of crimped steel fibres. Approximately 41.9% of increase in first crack load is achieved with 10.5% of increase in ultimate load carrying capacity pertaining to deep beam at 1% steel fibre content. The maximum deflection of the DB-T specimens did not exhibit a strictly monotonic trend with increasing CSF content. Intermediate fluctuations were observed; however, the maximum deflection decreased overall from 3.08 mm for the specimen without CSF to 2.70 mm at 1% CSF, corresponding to a reduction of 12.34%. The observed fluctuations may be associated with experimental variability arising from random fibre distribution and orientation, localized stress concentration around the tension-zone openings, variation in diagonal crack paths and differences in fibre-bridging efficiency.

Table 7. Load – Deflection pertaining to deep beam with opening in tension zone for various CSF content

Percentage of crimped steel fibres (%)	Number of specimens	DB-T		
		Mean First Crack Load (kN)	Mean Ultimate Load (kN)	Mean Maximum Deflection (mm)
0	3	62	152	3.08
0.25	3	67	156	3.00
0.50	3	72	158	3.14
0.75	3	82	166	3.34
1.00	3	88	168	2.70

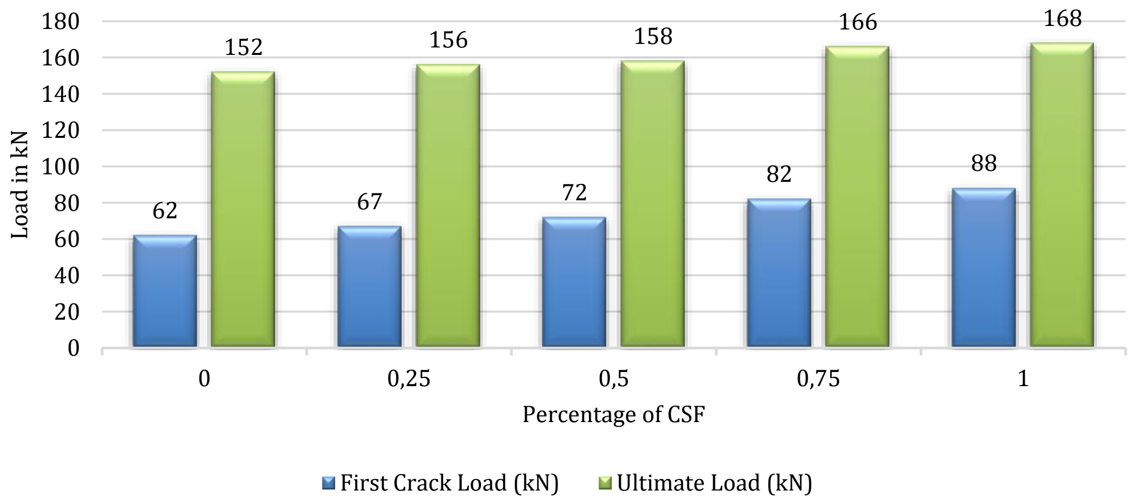

Fig. 10. First crack load and ultimate load for DB-T

The relative assessment of all three types of beam configuration demonstrates that the solid deep beam (SDB) exhibits the highest structural performance, followed by beam having circular web opening made in compression zone (DB-C), while the deep beam with circular web opening in tension zone (DB-T) recorded the lowest load resisting capacity. The placement of circular opening in the compression zone (DB-C) results smaller reduction in first crack load of about 4% and ultimate load of 2.8% while placing the opening in tension zone (DB-T) results in higher reduction of first crack load of 12% and ultimate load of 6.7% when compared with solid beam without opening (SDB)

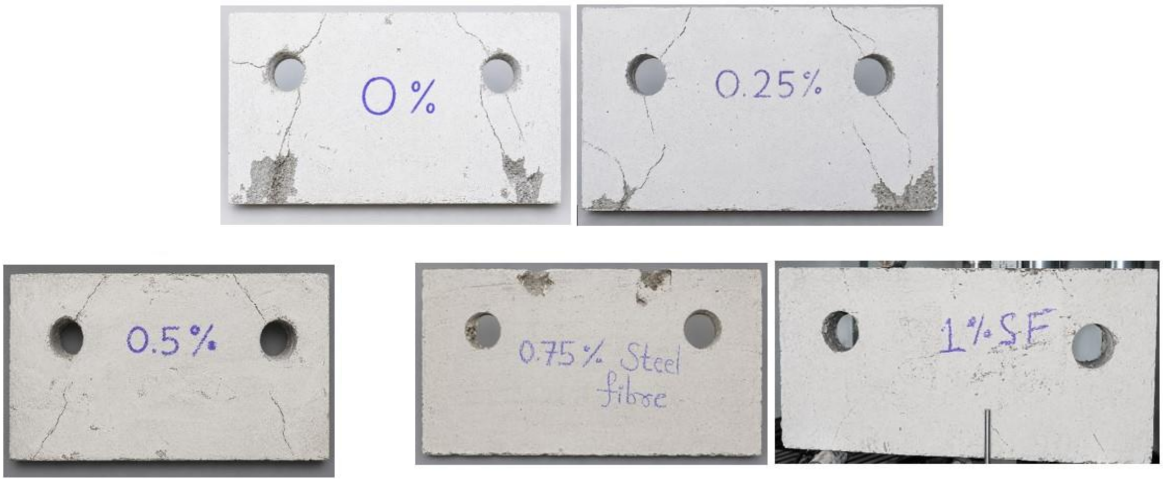

Fig. 11. Failure patterns of DB-C specimens with different CSF contents at ultimate load

The above figure 11 presents the representative post-failure crack pattern of DB-C specimens with different CSF contents, ranging from 0% to 1%. The figure 11 is provided to illustrate the development and propagation of cracks around the circular web openings and the influence of increasing CSF content on the failure behavior. Similar observations were recorded for the SDB and DB-T specimens.

7.4 Theoretical Formula to Find Ultimate Shear Strength of the Deep Beams

According to Professor F. K. Kong [19], the expression for the factored shear-resisting capacity pertaining to deep beam is given by equation below:

$$Qu/bD = (Pu/2bD) = \xi 1[0.1\, fc\, (\lambda 1)\, (\lambda 2)\, (\lambda 3) + 0.0085\, \Psi_s\, ps\, f_{sy} + 0.01\, \Psi_w\, K_w\, r_w\, f_{wy}] \tag{3}$$

Where; Q_u = ultimate shear bearing with single concentrated load, Pu/2 considered for two-point loading system. b = breadth pertaining to deep beam = 75 mm, D = Overall depth of beam = 325 mm, ξ_1 = performance factor or safety factor for beam failing in shear = 0.75, f_{sy}, f_{wy} = yield strength of longitudinal bar and web bar respectively (N/mm^2) for 12 mm diameter steel = 515 N/mm^2 and for 8 mm diameter steel = 510 N/mm^2. f_c **=** cylindrical (150 mm dia.×300 mm height) compressive strength of concrete, Ψs = empirical co-efficient = 0.65, Ψ_w = empirical co-efficient = 0.50. p_s = (A_s/bD) * 100, expressed in percentage = 0.928, r_w = (A_w/bD) * 100, expressed in percentage = 0.412, K_w = 0.50. λ_1, λ_2, λ_3 **=** empirical co-efficient of deep beam with and without openings based on opening parameters and mentioned in the table 8 below.

Table 8. Empirical co-efficient used for Professor F. K. Kong's formula for ultimate shear strength prediction

Parameters	SDB	DB-C	DB-T
λ1	1	0.88	0.67
λ2	1	1	1
λ3	0.72	0.55	0.52

Two-legged 8 mm diameter stirrups at 230 mm c/c were provided in SDB, DB-C and DB-T. Therefore, area of the two stirrups legs was A_w = 100.53 mm². Accordingly, r_w = (A_w/bD) x 100 = 0.412%. Hence, r_w = 0.412% was used for SDB, DB-C, DB-T. The configurations were differentiated through their respective λ_1, λ_2 and λ_3 coefficients. For example, at 0% CSF, using f_c = 17.60 N/mm², p_s = 0.928%, r_w = 0.412%, Ψ_s = 0.65, Ψ_w = 0.50 and K_w = 0.50, the theoretical ultimate loads were 162.08 kN for SDB, 146.90 kN for DB-C and 138.17 kN for DB-T. These were rounded to 162, 147 and 138 kN respectively, in Table 9.

Since the original Kong formulation was developed for conventional reinforced concrete deep beams and does not specifically account for the steel fibre volume fraction, the effect of increasing CSF content was considered indirectly through the fibre-modified concrete properties. In the present study, the experimentally determined cube compressive strengths for each CSF content were converted to equivalent cylindrical compressive strengths and incorporated into the theoretical calculation. Consequently, the theoretical model was used as a comparative approach to evaluate the influence of changes in fibre-modified concrete strength rather than a fibre-specified predictive model

Table 9. Theoretical ultimate load of deep beams with varying CSF contents

Percentage of crimped steel fibres (%)	SDB	DB-C	DB-T
	Ultimate Load (kN)	Ultimate Load (kN)	Ultimate Load (kN)
0	162	147	138
0.25	167	150	140
0.50	174	155	144
0.75	183	161	148
1.00	187	164	150

The theoretical prediction obtained using developed analytical model provides good agreement with experimental results of crimped steel fibre reinforced concrete deep beam with and without circular web openings. A variation of 0.6% to 10.8% between the theoretical and experimental values indicates satisfactory agreement between two sets of results. The analytical model (theoretical values) provides a reasonably accurate prediction of the experimental ultimate load of steel fibre-reinforced concrete deep beams, including SDB, DB-C and DB-T. The maximum variation of results comparable with experimental work and theoretical values are about 10.8% and minimum variation is about 0.60%.

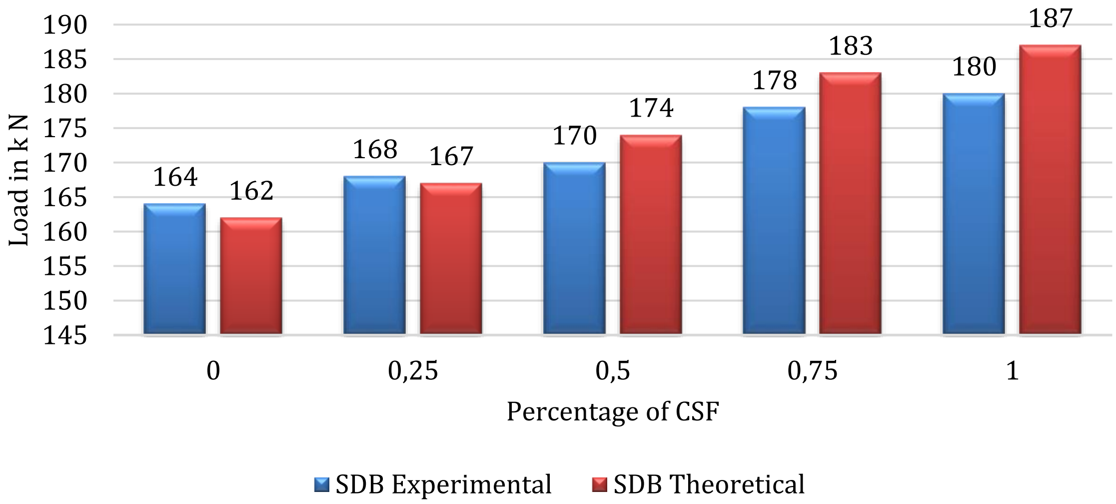

Fig. 12. Comparison of experimental and theoretical ultimate loads of SDB with varying CSF

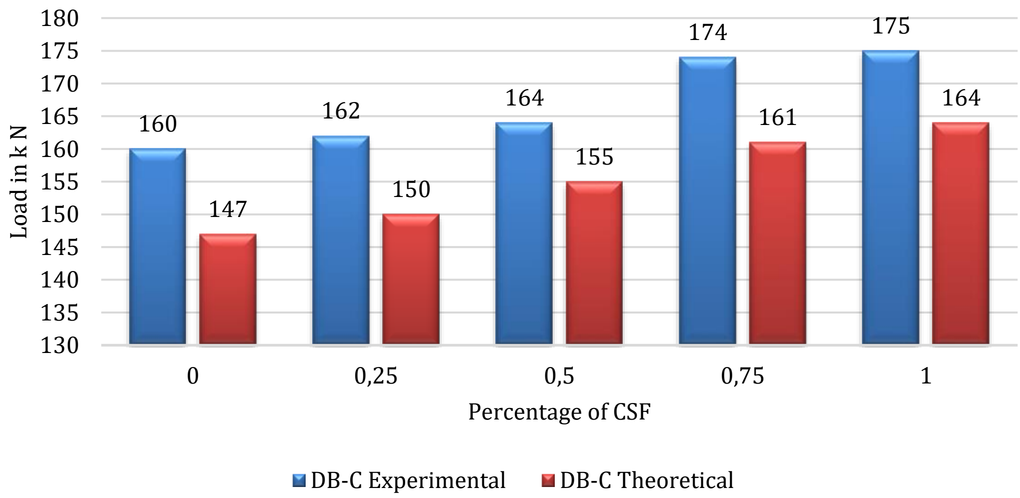

Fig. 13. Comparison of experimental and theoretical ultimate loads of DB-C with varying CSF

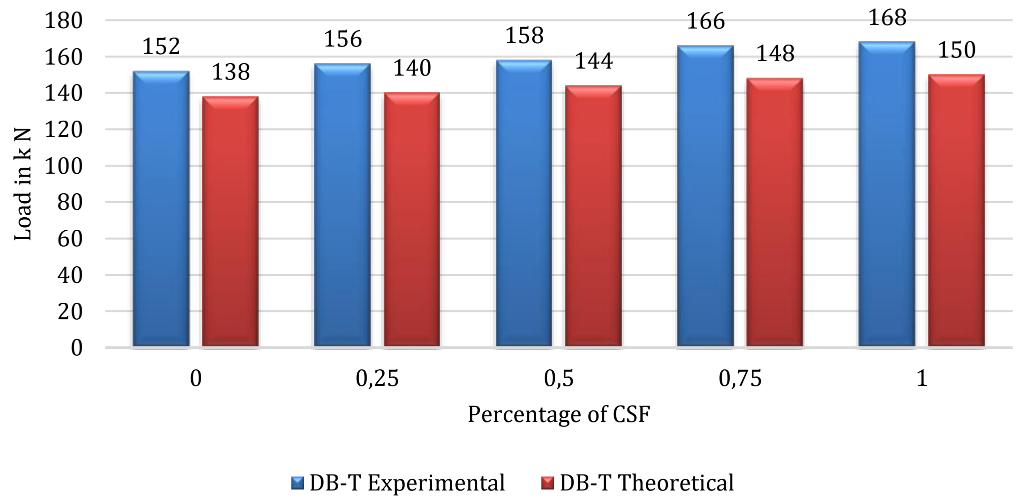

Fig. 14. Comparison of experimental and theoretical ultimate loads of DB-T with varying CSF

8. Conclusion

The introduction of circular web openings disrupted the natural load-transfer mechanism of the deep beams. Compared with SDB, DB-T exhibited a maximum reduction of 16.33% in the first-crack load at 0.75% CSF, decreasing from 98 kN to 82 kN. The maximum reduction in ultimate load-carrying capacity was 7.32% at 0% CSF, decreasing from 164 kN for SDB to 152 kN for DB-T. Across the investigated CSF contents, both DB-C and DB-T specimens exhibited crack development around the circular openings, with cracks extending towards the loading and support regions. These observations demonstrate the influence of opening location on the load-transfer mechanism and failure behavior of deep beams. The position of circular web opening relative to load path substantially influenced the structural behavior of specimens. Averaged over the five CSF contents, DB-C exhibited 8.34% and 4.38% higher first-crack and ultimate loads, respectively, than DB-T. At 1% CSF, DB-C also exhibited 9.09% and 4.17% higher first-crack and ultimate loads, respectively, than DB-T. These results indicate that positioning the circular opening in the compression zone was less detrimental than positioning it in the tension zone. The incorporation of CSF at volume fractions ranging from 0.25% to 1%, in increments of 0.25%, improved the first-crack and ultimate loads compared with the corresponding specimens without CSF. At 1% CSF, SDB exhibited increases of 35.14% (26 kN) in the first-crack load and 9.76% (16 kN) in the ultimate load. The corresponding increases for DB-C were 41.18% (28 kN) and 9.38% (15 kN), respectively, while DB-

T exhibited increases of 41.94% (26 kN) and 10.53% (16 kN), respectively. The improved response was attributed to the crack-bridging action of CSF, which restrained crack propagation and enhanced load transfer after cracking. Among the investigated CSF fibre volume fractions, 1% CSF provided the greatest improvement in load-carrying performance. The theoretical ultimate-load predictions showed reasonable agreement with the experimental results, with variations ranging from 0.6% to 10.8%. This agreement supports the applicability of Kong's model for estimating the ultimate shear-carrying capacity of the tested CSF-reinforced concrete deep beams with circular web openings. However, its applicability should be limited to the investigated material properties, specimen dimensions, opening geometry and loading conditions until further experimental validation is available.

9. Limitations and Future Scope

- The width of the designed reinforced members (75 mm) used in this study may introduce scale effects, and the laboratory-scale specimens may not be fully representing full-scale behavior.
- The use of CSF can potentially reduce conventional shear reinforcement, thereby simplifying reinforcement fabrication and reducing labor and construction time. However, a detailed cost assessment is required to quantify the economic benefits.
- Future studies should investigate different opening positions, size and shapes such as square and rectangular openings.
- The influence of alternative fibre types, such as polypropylene, glass, basalt and synthetic fibres can be investigated in future studies

Acknowledgement

The authors acknowledge that this study is supported by Department of Civil Engineering, Nagarjuna College of Engineering and Technology, Bengaluru, Karnataka, India and SJC Institute of Technology, Chickballapur, Karnataka, India, for carrying out this research work. The author also thanks the technical and laboratory staff for their assistance during specimen preparation and experimental testing.

References

[1] Ghalla M, Elsamak G, El-Zohairy A, Youssf O, Khairy S, & Badr el-din A. Experimental investigation on the structural performance of strengthened reinforced concrete deep beams using steel-based and SHCC techniques. Structures, 2026, 85: 111074. https://doi.org/10.1016/j.istruc.2026.111074

[2] Sogut K, Ercan B. Behaviour of unstrengthened and DE CFRP-strengthened high-strength concrete deep beams with web openings. Frontiers in Materials, 2025, 12: pp. 1-15. https://doi.org/10.3389/fmats.2025.1661180

[3] Kannan H, Veerappan S K and Sivasubramanian M V R. Experimental and numerical investigation of shear performance of RC deep beams strengthened with engineered cementitious composites. Construction Materials, 2025, 5(3), pp. 1-16. https://doi.org/10.3390/constrmater5030051

[4] Khalaf D, Chassib S M. Shear Behaviour of RC Deep Beams Made with Recycled Bricks: Comparative Study. Civil and environmental engineering, 2025, 21(2): pp. 788-811. https://doi.org/10.2478/cee-2025-0057

[5] Shallan M E, Khalil M, Mahmoud A and El-Diasity M H. Shear performance of continuous deep beams reinforced with steel, GFRP bars, stirrups, and novel grating system: an experimental study. Materials and Structures, 2025, 58(7): 231. https://doi.org/10.1617/s11527-025-02751-5

[6] Shabanlou M, et al. Experimental and analytical study of the residual performance of reinforced concrete deep beams with circular web openings. Results in Engineering, 2025, 25: 104229. https://doi.org/10.1016/j.rineng.2025.104229

[7] Abbas H, Al-Mahbashi M, Elsanadedy H, Abadel A, Almusallam T and Al-Salloum Y. Strengthening of high-strength RC continuous deep beams having rectangular web openings using bolted steel plates. Engineering Structures, 2025, 337: 120519. https://doi.org/10.1016/j.engstruct.2025.120519

[8] Daudi S A. Shear performance of deep concrete beams with openings using waste tyre steel fibres: FEM and ANN analysis. Civil Engineering Journal, 2024, 10(8): pp. 2422-2449. https://doi.org/10.28991/CEJ-2024-010-08-02

[9] Hasan AF, Al Amlin AS. Shear strengthened of R.C hollow deep beams with large opening by plates: A Review. Al-Rafidain Journal of Engineering Sciences, 2025, 3(1):89-112. https://doi.org/10.61268/mcvakq81

[10] Mona S, Mohammad A, Mohamed Zakaria. Shear capacity prediction for reinforced concrete deep beams with web openings using artificial intelligence methods. Engineering Structures, 2023, 280: 115675. https://doi.org/10.1016/j.engstruct.2023.115675
[11] Farouk M A, Moubarak A M, Ibrahim A and Elwardany H. New alternative techniques for strengthening deep beams with circular and rectangular openings. Case Studies in Construction Materials, 2023, 19: e02288. https://doi.org/10.1016/j.cscm.2023.e02288
[12] Nancy K, Tamer E, Hilal E, Bilal E. Shear response of recycled aggregates concrete deep beams containing steel fibres and web openings. Sustainability, 2022, 14(2): 945. https://doi.org/10.3390/su14020945
[13] Waleed A J, Abbas A and Nazar K A. Effect of size and location of square web openings on the entire behavior of reinforced concrete deep beams. Civil Engineering Journal, 2019, 5(1): pp. 209-226. https://doi.org/10.28991/cej-2019-03091239
[14] Moradi M, Reza M. Application of the strut-and-tie method for steel fiber reinforced concrete deep beams. Construction and Building Materials, 2016, 131:423-437. https://doi.org/10.1016/j.conbuildmat.2016.11.042
[15] Azharuddin N H, Pankaj B. Experimental Evaluation Shear Strength of Steel Fibre Reinforced Concrete Deep Beam. International Journal of Engineering Research & Technology, 2016, 5(5): pp. 97-106.
[16] Ahmed S, Ihsan A S, Sabih Z. Effect of steel fiber on the behavior pertaining to deep beams with and without web opening. Engineering and Technology Journal, 2011, 29(1): pp. 1-19.
[17] Naik U, Kute S. Span-to-depth ratio effect on shear strength of steel fiber reinforced high-strength concrete deep beams using ANN model. International Journal of Advanced Structural Engineering (IJASE), 2013, 5(1): 29
[18] Vengatachalapathy V, Ilangovan R. A Study on Steel Fibre Reinforced Concrete Deep Beams With and without Openings. International Journal of Civil and Structural Engineering, 2010, 1(3): pp. 509-517.
[19] Kong F K. Reinforced concrete deep beams. CRC Press, 1990.
[20] Shetty M S, Jain A K. Concrete Technology: Theory and Practice. 8th edition New Delhi, India, S Chand Publishing, 2019.